Biomechanical analysis of practitioner's gesture for peripheral venous catheter insertion

Kévin Torossian, Mélanie Ottenio, Anne Catherine Brulez, Yoann Lafon, Anthony Viste, Patrick Attali, Stéphane Benayoun

▶ **To cite this version:**

Kévin Torossian, Mélanie Ottenio, Anne Catherine Brulez, Yoann Lafon, Anthony Viste, et al.. Biomechanical analysis of practitioner's gesture for peripheral venous catheter insertion. Medical Engineering & Physics, 2021, 90, pp 92-99. 10.1016/j.medengphy.2021.03.001 . hal-03187576

HAL Id: hal-03187576
https://hal.science/hal-03187576

Submitted on 15 Mar 2023

HAL is a multi-disciplinary open access archive for the deposit and dissemination of scientific research documents, whether they are published or not. The documents may come from teaching and research institutions in France or abroad, or from public or private research centers.

L'archive ouverte pluridisciplinaire **HAL**, est destinée au dépôt et à la diffusion de documents scientifiques de niveau recherche, publiés ou non, émanant des établissements d'enseignement et de recherche français ou étrangers, des laboratoires publics ou privés.

Distributed under a Creative Commons Attribution - NonCommercial 4.0 International License

Version of Record: https://www.sciencedirect.com/science/article/pii/S1350453321000242
Manuscript_9c234a563019c6f649de1855d578f194

Biomechanical analysis of practitioner's gesture for peripheral venous catheter insertion

K. Torossian[a,b 1], M. Ottenio[b], A-C. Brulez[c], Y. Lafon[b], A. Viste[b,d], P. Attali[e], and S. Benayoun[a]

[a] *Laboratoire de Tribologie et Dynamique des Systèmes, UMR CNRS 5513, Ecole Centrale de Lyon, 36 avenue Guy de Collongues, 69134 Ecully, France.*
[b] *Univ Lyon, Université Claude Bernard Lyon 1, Univ Gustave Eiffel, IFSTTAR, LBMC UMR_T9406, F69622, Lyon, France*
[c] *Laboratoire de Génie de la Fonctionnalisation des Matériaux Polymères, Institut Textile et Chimique de Lyon, 87 chemin des Mouilles, 69134 Ecully cedex, France.*
[d] *Hospices Civils de Lyon, Hôpital Lyon Sud, Chirurgie Orthopédique, 165 Chemin du Grand Revoyet, 69495 Pierre Benite Cedex, France.*
[e] *Institut de Formation en Soins Infirmiers, 5 Avenue Esquirol, 69003 Lyon, France.*

Abstract

Peripheral venous catheter insertion (PVCI) is one of the most common procedures performed by healthcare professionals but remains technically difficult. To develop new medical simulators with better representativeness of the human forearm, an experimental study was performed to collect data related to the puncturing of human skin and a vein in the antebrachial area. A total of 31 volunteers participated in this study. Force sensors and digital image correlation were used to measure the force during the palpation and puncturing of the vein and to retrieve the kinematics of the practitioner's gesture. The *in vivo* skin rupture load, vein rupture load, and friction loads for skin only and for both the skin and vein were (mean ± standard deviation) 0.85 ± 0.34 N, 1.25 ± 0.37 N, –0.49 ± 0.19 N, and –0.51 ± 0.16 N, respectively. The results of this study can be used to develop realistic skin and vein substitutes and mechanically assess them by reproducing the practitioner's gesture in a controlled fashion.

Keywords: peripheral venous catheter insertion, puncture, palpation, skin, vein

1. Introduction

When the oral route cannot be used, peripheral venous catheter insertion (PVCI) is performed to administer intravenous therapy, e.g., medication and fluids. This medical procedure consists of five main phases: (1) palpation to locate the superficial vein to puncture, (2) disinfection of the area to puncture, (3) skin stretching to prevent the vein from rolling by applying a normal and tangential force, (4) skin and vein puncture, and (5) catheter placement followed by withdrawal of the needle [1].

Although PVCI is one of the most common procedures performed by healthcare professionals, it remains technically difficult. Studies indicated that the success rates ranged between 44% and 76.9% for young nurses and between 91% and 98% for nurses with more education and experience [2–4]. Medical simulators are commonly used by healthcare students during their training, before their first procedure on a real patient. However, the haptic feedback of current simulators remains vastly

[1] Corresponding author: Laboratoire de Tribologie et Dynamique des Systèmes, UMR CNRS 5513, Ecole Centrale de Lyon, 36 Avenue Guy de Collongues, 69134 Ecully cedex, France.
E-mail address: kevin.torossian@ec-lyon.fr

© 2021 published by Elsevier. This manuscript is made available under the CC BY NC user license
https://creativecommons.org/licenses/by-nc/4.0/

different from the actual sensation of touch and perforation, reducing the immersivity of the simulation experience.

To design more realistic PVCI simulators, attention should be paid to reproducing the mechanical response of the forearm's skin and vein during *in vivo* PVCI. As mentioned previously, the two main loadings performed by the practitioner are palpation, which is comparable to an indentation test from a mechanical viewpoint, and perforation.

Indentation tests reported in the literature indicated that multilayered and viscoelastic materials such as skin [5] are significantly influenced by the observation scale [6] and the loading speed [7]. Similarly, the force needed to puncture soft tissues depends on several parameters [8], such as the penetrator geometry, tissue state, anatomical area, and loading parameters (velocity, angle insertion, level of pre-stretching of the tissue). Therefore, for evaluating the realism of potential synthetic surrogates for PVCI, the boundary conditions for *in vivo* PVCI must be quantified to experimentally reproduce the practitioner's gesture.

A literature review [9] collected results from different studies all concerned with soft tissues perforation by a needle. The peak loads were given as well as an indication of the anatomical area, the perforator diameter, the insertion velocity and its angle. Among the cited papers, the work of Shergold and Fleck [10] can be highlighted in regard with our application. They performed perforation on *in vivo* human skin in the antebrachial area by driving a hand-operated instrument making a 90° angle with the forearm at 1 $mm.s^{-1}$. Okuno et al. [11] is also of great interest since they developed an instrumented syringe, so that puncture of the *in vivo* superficial veins of the ventral forearm could be performed by a medical technician. Insertion velocity and angle were respectively estimated at 15 $mm.s^{-1}$ and 15°, although no measurements were made. However, the tissues were probably solicited mechanically in the same way as they would be during a PVCI on a patient. Both of the mentioned studies reported rupture loads of either only skin or only vein which were respectively measured between 0.6 – 0.8 N [10] and 0.14 – 0.87 N [11].

However, relying solely on rupture loads to mimic the sensation of perforation with tissue mimicking substitutes is probably not enough to get a realistic haptic feedback. Indeed, Okamura et al. [12] stated that needle insertion is characterized by a summation of stiffness, friction and cutting forces. The stiffness force occurs before puncture, while friction and cutting forces occur after puncture. So, friction and cutting forces should also be considered. Yet, none of the aforementioned results obtained on *in vivo* ventral forearm were capable of decomposing the different loads applied on the needle during puncture, because only the insertion phase was recorded.

Here, an experimental setup was developed to record both the spatial coordinates and the load applied by the practitioner during palpation and perforation.

The remainder of this paper is organized as follows. First, the proposed method for capturing the gesture and load applied to the forearm during palpation and perforation is described. Second, kinematics and load measurements for each step of the medical procedure are reported. Finally, the results are compared with those reported in the literature, and recommendations are provided for future research.

2. Materials and methods

2.1. Volunteer panel

PVCI was performed on the ventral forearms of 31 healthy volunteers by an experienced nurse instructor (29 years of experience). The participants included 8 women and 11 men in the age range of 18–25 years and 11 women and 1 man in the age range of 60–75 years. Among them, three young and three elderly volunteers were obese. The age difference between the groups was selected according to the experience of the practitioner, who reported that the sensation of skin and vein puncture changes slightly at approximately 60 years of age. This study was approved by the research ethics committee "Comité de protection des personnes" of Ile-de-France V and the National Agency of Medicines Security under the reference number 2018-A02895-50.

2.2. Kinematics recording

The medical gesture was recorded by two high-speed cameras (FASTCAM SA3, Photron, Japan) at 125 frames per second. The self-adhesive targets located on the side of the palpating finger and an instrumented syringe were tracked using digital image correlation (DIC) software (VIC 3D® - Correlated Solution). The cameras were calibrated using a calibration chart and the DIC software before each day of testing.

Using the recorded coordinates, the displacement amplitude and instantaneous velocity of the palpating finger were determined, along with the needle insertion velocity during perforation. As palpation is a cyclical motion, the mean of the maximum displacement for each palpation motion was computed for each volunteer. The maximum displacement was determined by subtracting the initial contact position of the practitioner's finger on the volunteer's forearm from the position of the finger when it stopped pressing the forearm. The instantaneous velocity was calculated by dividing the position interval by the time for each frame of the video.

[INSERT FIGURE 1]

Figure 1: Explanatory scheme describing the projection of the instrumented syringe's targets on the forearm

An orthonormal plane called the "punctured plane" was constructed using self-adhesive targets taped in the vicinity of the punctured area. The insertion angle α was calculated by projecting the syringe vector $\overrightarrow{M_iN_i}$ (representing two targets on the instrumented syringe) onto the punctured plane. As the forearm is slightly curved, a bisector plane P of unit normal vector $\vec{n}$ was derived from two planes symmetrically opposed with respect to the proximal–distal axis of the forearm (Figure 1). P_1 was defined as a plane containing vectors $\overrightarrow{AB}$ and $\overrightarrow{AC}$, and P_2 was defined as a plane containing vectors $\overrightarrow{DC}$ and $\overrightarrow{DE}$. The unit normal vectors $\overrightarrow{n_1}$ and $\overrightarrow{n_2}$ were obtained by taking the cross product of the planes' guiding vectors. Then, the cross product and the scalar product of vectors $\overrightarrow{n_1}$ and $\overrightarrow{n_2}$ yielded the guiding vectors $\vec{x}$ and $\vec{y}$ of the bisector. Finally, the cross product of $\vec{x}$ and $\vec{y}$ yielded $\vec{n}$, thus enabling to derive Eq. 1:

$$\alpha = arcsin\left(\frac{\left\|\overrightarrow{M_iN_i}.\vec{n}\right\|}{\left\|\overrightarrow{M_iN_i}\right\|}\right). \quad \text{Eq. 1}$$

2.3. Palpation-load measurements

During the palpation of the ventral forearm to localize the vein to puncture, the load was measured using a 4.4-N flexible piezoresistive sensor (FlexiForce® A201–L, Mescan®) placed on the tip of the palpating finger (Figure 2.a).

[INSERT FIGURE 2]

Figure 2: a) Piezoresistive sensor placed on the palpating finger of the practitioner; b) sensitive area of the sensor surrounded by a semi-rigid silicone disk and a metallic puck

The sensor had a built-in sensitive area on which a semi-rigid silicone disk was placed to uniformly distribute the reaction force. Additionally, a metallic puck was fixed on the other side of the sensitive area to minimize the deformation of the fingertip during palpation (Figure 2.b). For each PVCI, the sensor was attached to the fingertip with double-sided adhesive tape and maintained by a medical glove. The double-sided tape was changed as soon as adhesion between the fingertip and the sensor became sub-optimal due to sebum secretion or sweat. The flexible sensor was then connected to a miniature WiFi transmitter to transfer data acquired at 200 Hz. This transmitter was fixed on the wrist of the practitioner by using a compression arm sleeve. The sensor was calibrated with different weights (50, 100, 200, and 300 g) before each half-day of testing to ensure a calibration score of $R^2 > 0.95$. Finally, the peak load was observed for each palpation motion for each volunteer (*i*) (Figure 3)

$$L_{P_i} = \frac{\sum_{j=1}^{m} L_{p_{i,j}}}{m}, \qquad \text{Eq. 2}$$

to determine the average maximum palpation load (Eq. 2):

where m represents the number of peak loads observed when palpation was performed on a volunteer, and $L_{P_{i,j}}$ represents the load for volunteer *i* and palpation *j*.

[INSERT FIGURE 3]

Figure 3: Typical palpation load ($L_{P_{i,j}}$) vs. time curve indicating each palpation load applied to the forearm of a volunteer

2.4. Puncture-load measurements

The skin and vein puncture loads were measured using an instrumented syringe specifically designed for this study (Figure 4). The device was composed of a 3D-printed casing, wherein a miniature 5-N load sensor was enclosed (LSB 200-5N, Andilog, France). A conical fitting was fixed to the sensor so that the catheter (20 Gauge, 20G) could be directly connected by wrapping its extremity with a finger cot to increase the friction. This allowed the device to maintain the needle and catheter assembly during its withdrawal while preventing blood from tainting the device. Sterile skin closure dressing strips were used to keep the needle and the catheter together and counter the influence of soft-tissue friction, which can withhold the catheter during withdrawal from the forearm

(Figure 4.b). Finally, the puncture loads and kinematics recordings were synchronized using a trigger switch connected to the cameras and the instrumented syringe.

[INSERT FIGURE 4]

Figure 4: a) Photograph and b) schematic of the instrumented syringe

As reported by [9], the needle insertion force is the sum of the stiffness, friction, and cutting forces (Eq. 3 2). The stiffness force occurs before puncturing, and the friction and cutting forces occur after puncturing. Thus, we can expect various levels of these forces for layers of different materials, with

$$f_{needle}(x) = f_{stiffness}(x) + f_{friction}(x) + f_{cutting}(x) \quad \text{Eq. 3}$$

the friction increasing as the needle passes through the materials.

To improve the accuracy of the force estimation, the vein depth can be estimated using the needle displacement (U_{skin}, U_{vein}) between the load peaks (Figure 5), which corresponds to skin and vein rupture, and the insertion angle α by employing basic trigonometry (Eq. 4).

[INSERT FIGURE 5]

Figure 5: Schematic of vein-depth computation: α represents the insertion angle, U_{skin} represents the needle position during contact with the skin, and U_{vein} represents the needle position during contact with the vein

$$insertion\ depth = \sin\alpha * |U_{skin} - U_{vein}| \quad \text{Eq. 4}$$

2.5. Experiment

Prior to testing, the volunteers were informed about the purpose of the study; their written informed consent was obtained. Then, they were examined by a physician to check whether they met the inclusion/exclusion criteria. The inclusion criteria were as follows:

- Age of 18–35 years or 60–75 years;
- Normal weight (18.5 ≤ Body Mass Index (BMI) ≤ 25) or obese (BMI ≥ 30).

The exclusion criteria were as follows:

- Bleeding disorders;
- Skin lesions, scars, and arteriovenous fistula in the ventral forearm;
- A high risk of infection;
- Women who had a lymph-node dissection on a malignant breast tumor;
- Declined cognitive function;
- Pregnancy or lactation;
- Participating in another study with an exclusion period;

- Medical history of fainting.

After it was confirmed that they satisfied the criteria, the volunteers sat on a blood sampling chair, with their right arms shifted toward the cameras. First, the practitioner palpated their forearms using only a tourniquet, both to identify the vein to puncture and to fix the camera shot. Once the vein was located, the palpation gesture was recorded, and the corresponding loads were measured. Then, the orthonormal plane composed of self-adhesive targets and used to compute the insertion angle was taped to the puncture site to be recorded. Finally, the plane was removed, the puncture site was disinfected, and puncturing was performed using the instrumented syringe.

3. Results

3.1. Palpation step

The average palpation velocity (V_{P_i}), peak load (L_{P_i}), and maximum palpating-finger displacement (D_{P_i}) were obtained for each volunteer (*i*) to calculate the average of the averages (Table 1).

Table 1 ***Results obtained from the biomechanical analysis of palpation***

	Average palpation velocity (mm/s)	**Average peak load (N)**	**Average maximum finger displacement (mm)**
Mean ± standard deviation	14.21 ± 4.32	0.15 ± 0.08	2.02 ± 0.82

The results were analyzed according to age and sex, as shown in Figure 6. On average, the palpation velocity was higher for men than for women and was higher for younger volunteers. Regarding age, the average maximum displacement of the palpating finger was significantly larger for the elderly volunteers, whereas the average palpation peak load was similar between the old and young groups.

[INSERT FIGURE 6]

Figure 6: Box plots illustrating the effects of age and sex on palpation: a) velocity; b) peak load; c) maximum finger displacement

The results in Table 1 are useful for reproducing the palpating gesture on skin substitutes, to mechanically compare them with human forearms under realistic conditions.

3.2. Puncture kinematics

As shown in Figure 7, the insertion angle was not constant during the puncture tests. The practitioner first increased the insertion angle to penetrate the skin and then gradually decreased it to insert the needle–catheter assembly into the vein while attempting not to puncture the vein's inner wall. Plotting the puncture load together with the insertion angle revealed that the insertion depth between the skin and the vein punctures was within the vein-depth range reported in the

literature. In a previous study [10], the depth of superficial veins in the forearm was estimated to be 1–3 mm via infrared imaging. The mean insertion angle and puncture velocity are presented in Table 2. Such results can be used in the design of venipuncture robots that mimic the gestures of medical professionals.

[INSERT FIGURE 7]

Figure 7: Example graph of the insertion angle and puncture load vs. the insertion depth

Table 2	***Results obtained from the analysis of the puncture gesture***	
	Mean puncture velocity (mm/s)	**Mean insertion angle (°)**
Mean ± SD	10.8 ± 2.1	15.3 ± 5.9

3.3. Puncture loads

PVCI was performed on 30 volunteers. For four of the volunteers, only the skin was punctured, because the practitioner missed the vein. Additionally, for five volunteers, the measured friction load was excluded from the analysis, because the catheter remained in the vein during the withdrawal phase. Figure 8 shows a typical load vs. time curve for the puncturing of a superficial vein in the forearm. This curve can be decomposed into sections corresponding to the different steps comprising the PVCI.

a) From A to B: The load increased owing to the skin stiffness until skin rupture, which occurred when the catheter penetrated the skin.
b) From B to C: The catheter progressed until it touched the vein; i.e., the load increased until the vein wall ruptured.
c) From C to D: The practitioner stopped the gesture and applied a cotton pad to stop the bleeding.
d) From D to E: The tissue-relaxation phase was characterized by the absence of relative motion between the needle and the tissues (only the static friction acting on the needle shaft was present).
e) From E to F: The catheter was withdrawn from the vein.
f) From F to G: The catheter was withdrawn from the skin.

[INSERT FIGURE 8]

Figure 8: Typical load vs. time curve obtained by puncturing the skin and vein of a human forearm using a 20G catheter

The skin and vein rupture loads, as well as the friction loads, are presented in Table 3. The friction loads were affected by the types of tissues in contact, the results are separated depending on whether the vein was punctured.

Table 3 Results obtained from the biomechanical analysis of perforation

	Skin rupture load (N)	Vein rupture load (N)	Friction load (N)	
			Vein and skin	Skin only
Mean ± SD	0.85 ± 0.34	1.25 ± 0.37	–0.51 ± 0.16	–0.49 ± 0.19

Figure 9 presents the differences in puncturing with regard to sex and age. Sex did not appear to influence the puncture loads at the forearm site (Figure 9.a), whereas age affected the vein rupture loads (Figure 9.b).

[INSERT FIGURE 9]

Figure 9: Box plots of puncture loads, illustrating the influences of a) sex and b) age

4. Discussion

The palpation gesture can differ among practitioners. While some practitioners only apply a normal force to the surface of the forearm to feel the bounciness of the vein, others apply shear stress to identify the vein. The latter gesture also helps to determine whether the vein can roll during puncturing. The flexible piezoresistive sensor used in this study to measure the normal force provided haptic feedback to the practitioner. In future studies, three-axis sensors can be investigated for determining the tangential loads. The average maximum displacement of the practitioner's finger depended significantly on the age of the subject, whereas the palpation peak load did not (Figure 6). These results can be explained by the variation of the Young's modulus of the skin, which has been shown to decrease by a factor of more than 2 between young and old populations [11].

The results for the mean displacement (Table 1)agree with the observations of Payne [12] who performed indentation tests on human skin. Payne reported that the subcutaneous fat tissues and underlying tissues have no influence on skin indentation for displacements of which are not exceeding 700 µm. This is consistent with the maximum displacement applied by the palpating finger, as the practitioner must feel the superficial veins to localize the area to puncture. Such displacement was applied in indentation tests in a few studies [13]. The researchers were thus able to evaluate the Young's modulus of the different layers of the skin and the underlying muscle. However, no study has been reported where indentation tests were performed to assess the effects of superficial veins on the mechanical response of the forearm. For the average palpation velocity and peak load, the obtained results were significantly higher than values reported in the literature, as the tests were performed in a quasi-static state, with an indentation speed and maximum normal load respectively lower than 1 mm/s and 60 mN, [11,14,15].

283

284 Table 4 shows rupture loads for different soft tissues reported in the literature review performed by
285 Torossian et al. [9]. Experimental conditions were also reported.

Table 4 ***Overview of published results for peak perforation during needle insertion in soft tissues*** [13]

References	Materials	Catheter	Insertion velocity (mm/s)	Insertion angle (°)	Perforator diameter (mm)	Peak force (N) (mean ± SD or range)
Abolhassani et al. [16]	Turkey skin and tissue	No	5–20	-	1.02	0.96 ± 0.063
Suzuki et al. [17] [a]	Polyethylene	Yes	3.3	30–45	0.09 1.02	0.12 0.27
	Lamb skin		1.67	30	-	3.4 ± 0.6 4.1 ± 0.2
Eriksson et al. [18] [b]	Latex	Yes	0.83	90	-	0.2
	In vivo human skin and dorsal hand vein		-	15–20	-	2.4 ± 0.9 3.5 ± 1.2
Shergold & Fleck [19]	*In vivo* human forearm skin	No	1	90	0.3 0.6	0.6 0.8
Podder et al. [20]	Perineal area *in vivo* male skin	No	300	90	1.47	15.03 ± 3.26
	Bovine muscle surrounded by chicken skin	No	100	-	-	4.4
Barbé et al. [21]	*In vivo* porcine skin	No	-	-	-	3
Zivanovic & Davies [22]	Polymer	No	-	30	-	1.5
Saito & Togawa [23]	*In vivo* rabbit ear and vein	No	2.5	15	0.4	0.18 ± 0.04
Kobayashi et al. [24]	Porcine jugular vein	No	5	20	1.36	0.52
Okuno et al. [25]	*In vivo* human forearm skin and median vein	No	15	15	0.4 0.8	0.23 ± 0.09 0.64 ± 0.23

[a] Peak forces correspond to needle insertion and catheter insertion.
[b] Peak forces were obtained for different catheter materials: PTFE and PUR.

286

Skin rupture loads measured in this study are consistent with results obtained by Shergold & Fleck [10] although experimental conditions were not similar. Measured vein rupture loads are relatively higher than those obtained by Okuno et al. [11] which could be explained, in our case, by the use of a larger gauge needle (20G).

As indicated by Table 3, the puncturing of superficial veins did not significantly increase the friction load, either because the wall was thin or because the contact friction was reduced by lubrification due to blood. Additionally, the vein rupture load was lower for older subjects (Figure 9), possibly owing to lower Young's moduli. A few volunteers with a BMI superior to 30 participated in the study. Obesity appeared to not affect the puncture loads; however, additional data are needed to confirm this.

To the best of our knowledge, this is the first paper to propose an analysis of the practitioner's gesture for PVCI, which can be now quantified with results shown in Table 2. The instrumented syringe affected the practitioner's gesture and thus the success rate, owing to the lack of haptic feedback through the needle tip. In future studies, researchers should aim to develop an instrumented syringe with enhanced haptic feedback.

None of the studies on *in vivo* forearm skin reported in the literature involved the decomposition of the load applied to the needle during puncturing, as only the insertion phase was recorded. In our study, the stiffness and friction forces were evaluated, and the cutting forces were neglected, as skin and veins can both be considered as thin membranes. Van Gerwen et al. [26] reviewed studies on needle–tissue interactions and proposed two types of crack growth processes that can occur on soft materials: stable (i.e., cutting) and unstable (i.e., rupture). They emphasized that for thin membranes, the amount of energy stored during the boundary displacement phase can be so large that a sudden crack extension occurs, forming a hole prior to the needle passing through the membrane thereby justifying the absence of cutting forces in this study.

One might also investigate whether the catheter surrounding the needle has a significant impact on the puncture curves, by changing the diameter or the friction comparing to stainless needle only. Eriksson et al. [18] performed PVCI with an instrumented syringe on *in vivo* dorsal veins of the hand, *in vitro* lamb skin membranes, and latex membranes. In their study, the catheter did not have a visible impact on the puncturing of human skin. However, for the lamb skin and latex membranes, peak loads were observed when the catheter top and tip were pushed through the membranes. Similarly, in our study, the catheter did not appear to affect the puncture measurements, indicating that its effects are only visible for stiffer materials.

The differences in the rupture loads with regard to age indicate that population-specific medical simulators must be designed to prepare students for different clinical situations. However, the differences may be too small to be haptically perceived by medical professionals and students. Therefore, venipuncture simulators should be developed with consideration of the tribology and subcutaneous properties, such as the vein prominence and tortuous or rolling veins.

5. Conclusion

A novel method was developed for the biomechanical analysis of the practitioner's medical gesture for PVCI. The kinematic analysis of palpation and puncture gestures can henceforth be used to mimic the practitioner's gestures. The average palpation and needle insertion velocities were 14.21 ± 4.32 mm/s and 10.8 ± 2.1 mm/s, respectively, and the average maximum finger displacement was 2.02 ± 0.82 mm. The visualization of the vein depth through the insertion angle, which had an average value of 15.3° ± 5.9°, provided a useful discriminative criterion for determining the vein rupture load.

Measured puncture loads can now be used to mechanically validate skin and vein substitutes. The skin rupture load, the vein rupture load, and the friction loads for the puncturing of the skin only and the puncturing of both the skin and vein were 0.85 ± 0.34 N, 1.25 ± 0.37 N, –0.49 ± 0.19 N, and –0.51 ± 0.16 N, respectively. Experimental results indicated that the age of the subject affected the vein rupture load, but further tests must be performed to confirm this.

Finally, the following question arises: to what extent does the instrumented syringe affect the haptic feedback of the practitioner and thus the venipuncture success rate? In future studies, different instrumented-syringe designs can be investigated to enhance the haptic feedback.

Acknowledgements

The authors thank Frederic Loprete for the design of the instrumented syringe and the volunteers for participating in the study. This study was sponsored and realized under the responsibility of Hospices Civils de Lyon. The tests were conducted in collaboration with UCBL and IFSTTAR, on their behalf and on behalf of the joint research unit Laboratoire de Biomécanique et Mécanique des Chocs (LBMC).

Ethical approval

The authorization for the study was granted by the ethic committee CPP of Ile-de-France V under the reference number 18.11.09.48602 and the National Agency of Medicines Security under the reference number 2018-A02895-50.

Funding

The author(s) disclosed receipt of the following financial support for the research, authorship, and/or publication of this article: this research was supported by ANR 11 IDFI 0034 as part of the SAMSEI project.

Conflicts of interest

The authors declare that they have no conflicts of interest.

References

[1] Beecham GB, Tackling G. Peripheral Line Placement. StatPearls, Treasure Island (FL): StatPearls Publishing; 2020.

[2] Frey AM. Success rates for peripheral i.v. insertion in a children's hospital. Financial implications. J Intraven Nurs 1998;21:160–5.

[3] Palefski SS, Stoddard GJ. The infusion nurse and patient complication rates of peripheral-short catheters. A prospective evaluation. J Intraven Nurs 2001;24:113–23.

[4] Jacobson AF, Winslow EH. Variables influencing intravenous catheter insertion difficulty and failure: an analysis of 339 intravenous catheter insertions. Heart Lung 2005;34:345–59.

[5] Dunn MG, Silver FH. Viscoelastic Behavior of Human Connective Tissues: Relative Contribution of Viscous and Elastic Components. Connective Tissue Research 1983;12:59–70.

[6] Kuilenburg J van, Masen MA, Heide E van der. Contact modelling of human skin: What value to use for the modulus of elasticity? Proceedings of the Institution of Mechanical Engineers, Part J: Journal of Engineering Tribology 2013;227:349–61.

[7] Fradet C, Lacroix F, Berton G, Méo S, Bourhis EL. Extraction des proprietes mecaniques locales d'un elastomere par nanoindentation : developpement des protocoles et application. Matériaux & Techniques 2017;105:109.

[8] Shergold OA, Fleck NA. Mechanisms of deep penetration of soft solids, with application to the injection and wounding of skin. Proceedings of the Royal Society of London A: Mathematical, Physical and Engineering Sciences 2004;460:3037–58.

[9] Okamura AM, Simone C, O'Leary MD. Force modeling for needle insertion into soft tissue. IEEE Trans Biomed Eng 2004;51:1707–16.

[10] Zharov VP, Ferguson S, Eidt JF, Howard PC, Fink LM, Waner M. Infrared imaging of subcutaneous veins. Lasers Surg Med 2004;34:56–61.

[11] Pailler-Mattei C, Debret R, Vargiolu R, Sommer P, Zahouani H. In vivo skin biophysical behaviour and surface topography as a function of ageing. J Mech Behav Biomed Mater 2013;28:474–83.

[12] Payne PA. Measurement of properties and function of skin. Clin Phys Physiol Meas 1991;12:105.

[13] Torossian K, Benayoun S, Ottenio M, Brulez A-C. Guidelines for designing a realistic peripheral venous catheter insertion simulator: A literature review. Proc Inst Mech Eng H 2019;233:963–78.

[14] Pailler-Mattei C, Bec S, Zahouani H. In vivo measurements of the elastic mechanical properties of human skin by indentation tests. Med Eng Phys 2008;30:599–606.

[15] Jachowicz J, McMullen R, Prettypaul D. Indentometric analysis of in vivo skin and comparison with artificial skin models. Skin Research and Technology 2007;13:299–309.

[16] Abolhassani N, Patel R, Moallem M. Experimental study of robotic needle insertion in soft tissue. International Congress Series 2004;1268:797–802.

[17] Suzuki T, Tanaka A, Fukuyama H, Nishiyama J, Kanazawa M, Oda M, et al. Differences in penetration force of intravenous catheters: effect of grinding methods on inner needles of intravenous catheters. Tokai J Exp Clin Med 2004;29:175–81.

[18] Eriksson E, Larsson N, Nitescu P, Appelgren L, Linder LE, Curelaru I. Penetration forces in cannulation of the dorsal veins of the hand: I. A comparison between polyurethane (Insyte®) and polytetrafluoroethylene (Venflon®) cannulae. Acta Anaesthesiologica Scandinavica 1991;35:306–14.

[19] Shergold OA, Fleck NA. Experimental investigation into the deep penetration of soft solids by sharp and blunt punches, with application to the piercing of skin. J Biomech Eng 2005;127:838–48.

[20] Podder TK, Sherman J, Clark DP, Messing EM, Rubens DJ, Strang JG, et al. Evaluation of robotic needle insertion in conjunction with in vivo manual insertion in the operating room. ROMAN 2005. IEEE International Workshop on Robot and Human Interactive Communication, 2005., 2005, p. 66–72.

[21] Barbé L, Bayle B, de Mathelin M, Gangi A. Needle insertions modeling: Identifiability and limitations. Biomedical Signal Processing and Control 2007;2:191–8.
[22] Zivanovic A, Davies BL. A robotic system for blood sampling. IEEE Trans Inf Technol Biomed 2000;4:8–14.
[23] Saito H, Togawa T. Detection of needle puncture to blood vessel using puncture force measurement. Med Biol Eng Comput 2005;43:240–4.
[24] Kobayashi Y, Hamano R, Watanabe H, Hong J, Toyoda K, Hashizume M, et al. Use of puncture force measurement to investigate the conditions of blood vessel needle insertion. Medical Engineering & Physics 2013;35:684–9.
[25] Okuno D, Togawa T, Saito H, Tsuchiya K. Development of an automatic blood sampling system: control of the puncturing needle by measuring forces. Proceedings of the 20th Annual International Conference of the IEEE Engineering in Medicine and Biology Society. Vol.20 Biomedical Engineering Towards the Year 2000 and Beyond (Cat. No.98CH36286), vol. 4, 1998, p. 1811–2 vol.4.
[26] van Gerwen DJ, Dankelman J, van den Dobbelsteen JJ. Needle-tissue interaction forces--a survey of experimental data. Med Eng Phys 2012;34:665–80.

Figure legend 1

Explanatory scheme describing the projection of the instrumented syringe's targets on the forearm

Figure legend 2:

a) Piezoresistive sensor placed on the palpating finger of the practitioner; b) sensitive area of the sensor surrounded by a semi-rigid silicone disk and a metallic puck

Figure legend 3:

Typical palpation load ($L_{P_{i,j}}$) vs. time curve indicating each palpation load applied to the forearm of a volunteer

Figure legend 4:

a) Photograph and b) schematic of the instrumented syringe

Figure legend 5:

Schematic of vein-depth computation: α represents the insertion angle, U_{skin} represents the needle position during contact with the skin, and U_{vein} represents the needle position during contact with the vein

Figure legend 6:

Box plots illustrating the effects of age and sex on palpation: a) velocity; b) peak load; c) maximum finger displacement

Figure legend 7:

Example graph of the insertion angle and puncture load vs. the insertion depth

Figure legend 8:

Typical load vs. time curve obtained by puncturing the skin and vein of a human forearm using a 20G catheter

Figure legend 9:

Box plots of puncture loads, illustrating the influences of a) sex and b) age

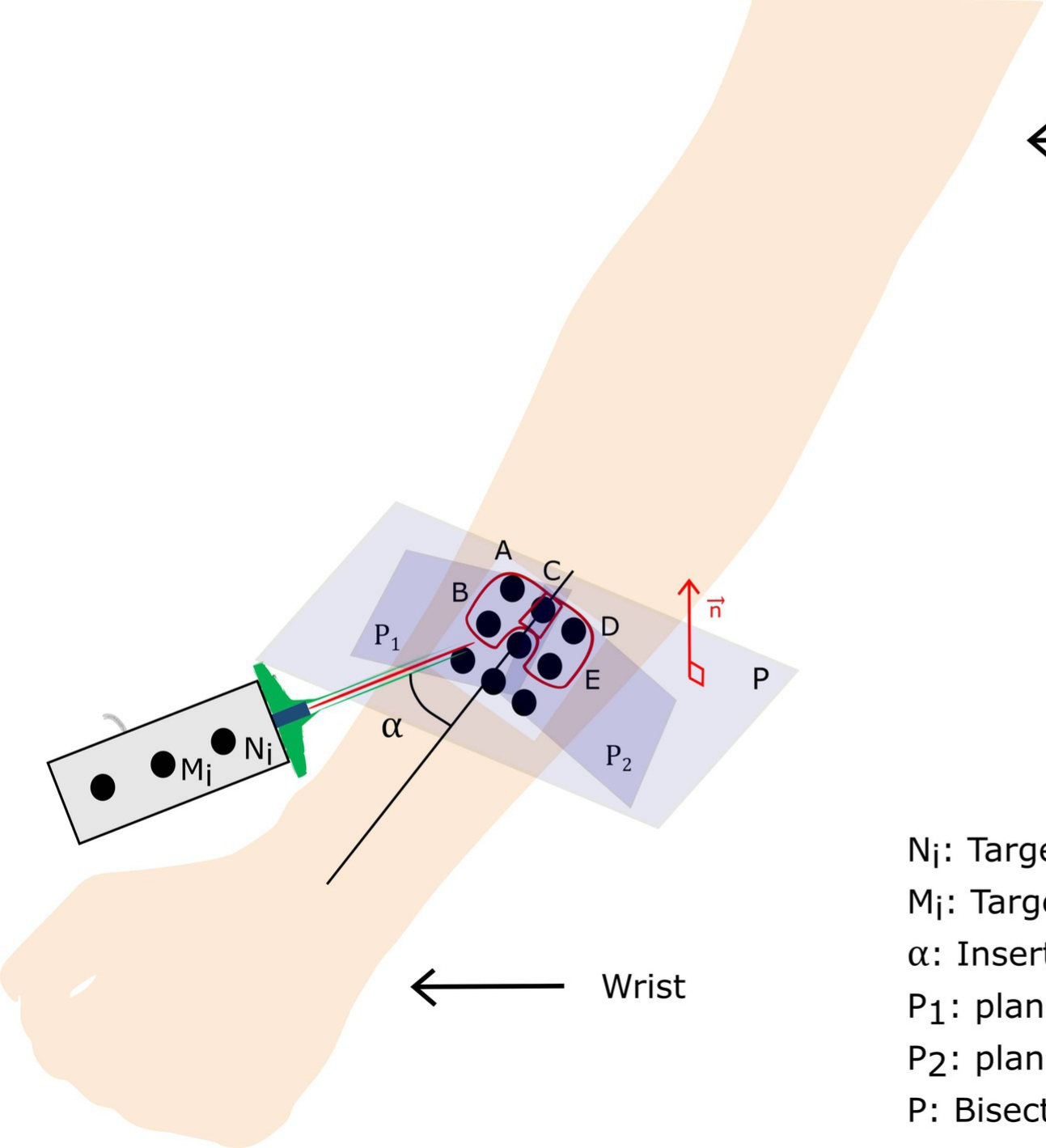

N_i: Target n°1 of the instrumented syringe

M_i: Target n°2 of the instrumented syringe

α: Insertion angle

P_1: plane formed by targets A, B, C

P_2: plane formed by targets C, D, E

P: Bisector plane of normal unit vector $\vec{n}$

a)

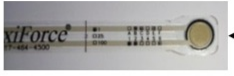

b)

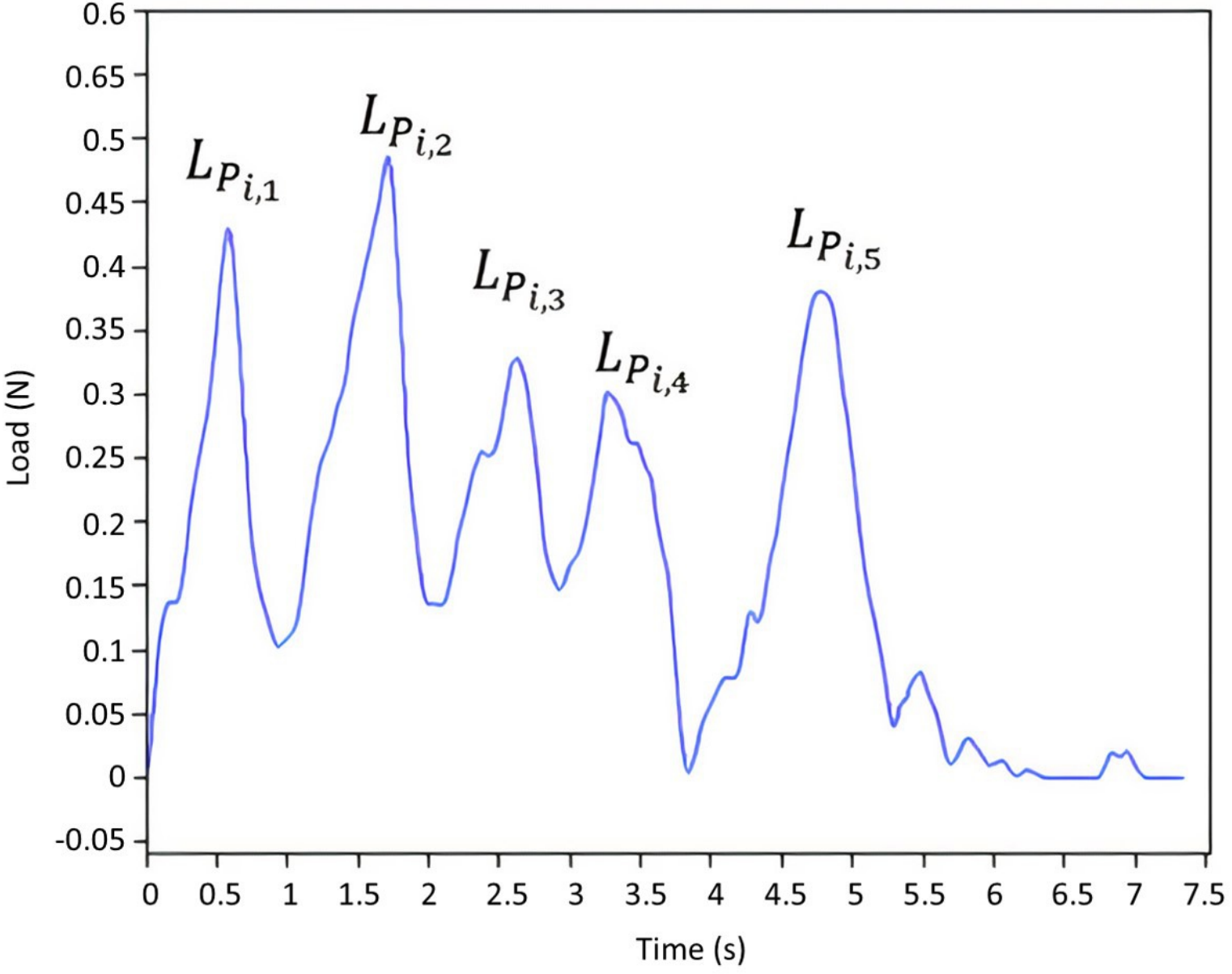
$L_{P_{i,1}}$
$L_{P_{i,2}}$
$L_{P_{i,3}}$
$L_{P_{i,4}}$
$L_{P_{i,5}}$
Load (N)
Time (s)
0.6
0.65
0.5
0.45
0.4
0.35
0.3
0.25
0.2
0.15
0.1
0.05
0
-0.05
0
0.5
1
1.5
2
2.5
3
3.5
4
4.5
5
5.5
6
6.5
7
7.5

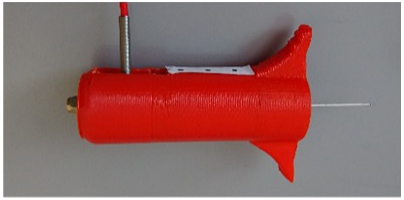

a)

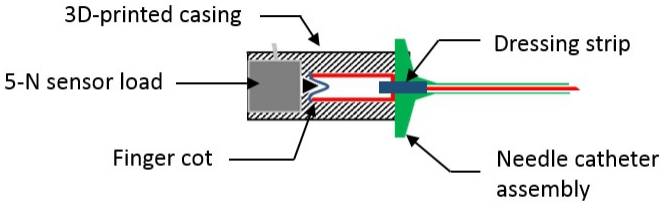
3D-printed casing
Dressing strip
5-N sensor load
Finger cot
Needle catheter assembly

b)

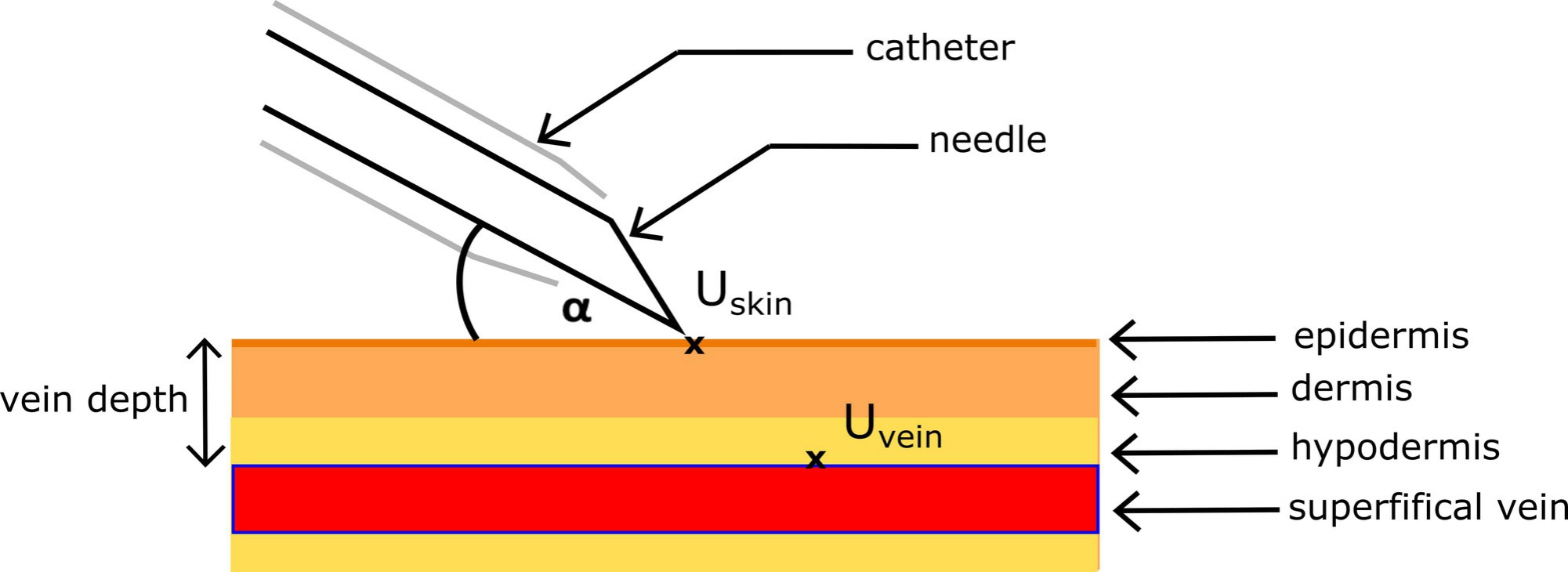
catheter
needle
α
U_{skin}
vein depth
U_{vein}
epidermis
dermis
hypodermis
superfifical vein

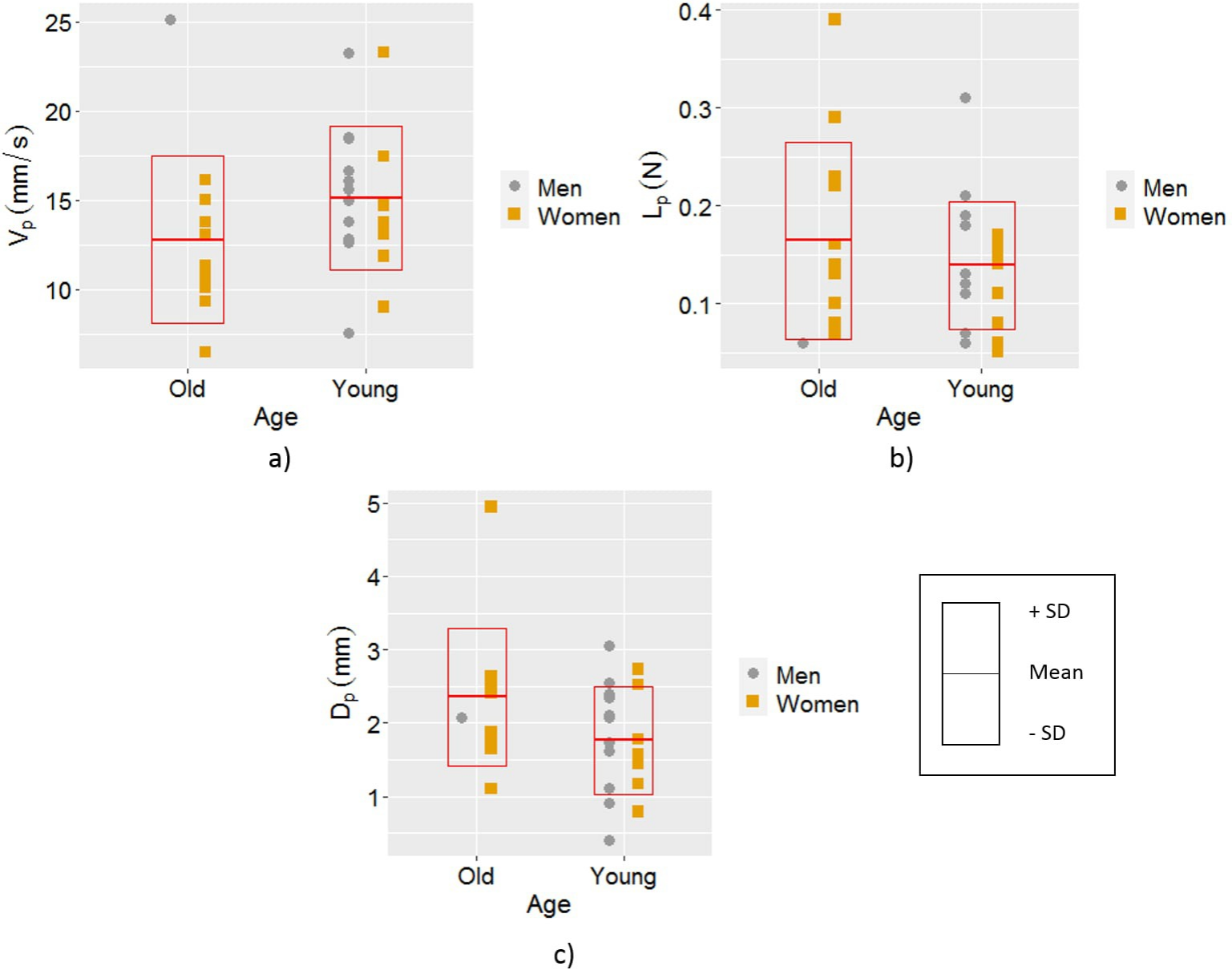
25
20
15
10
V_p (mm/s)
Old
Young
Age
Men
Women
a)
0.4
0.3
0.2
0.1
L_p (N)
Old
Young
Age
Men
Women
b)
5
4
3
2
1
D_p (mm)
Old
Young
Age
Men
Women
+ SD
Mean
- SD
c)

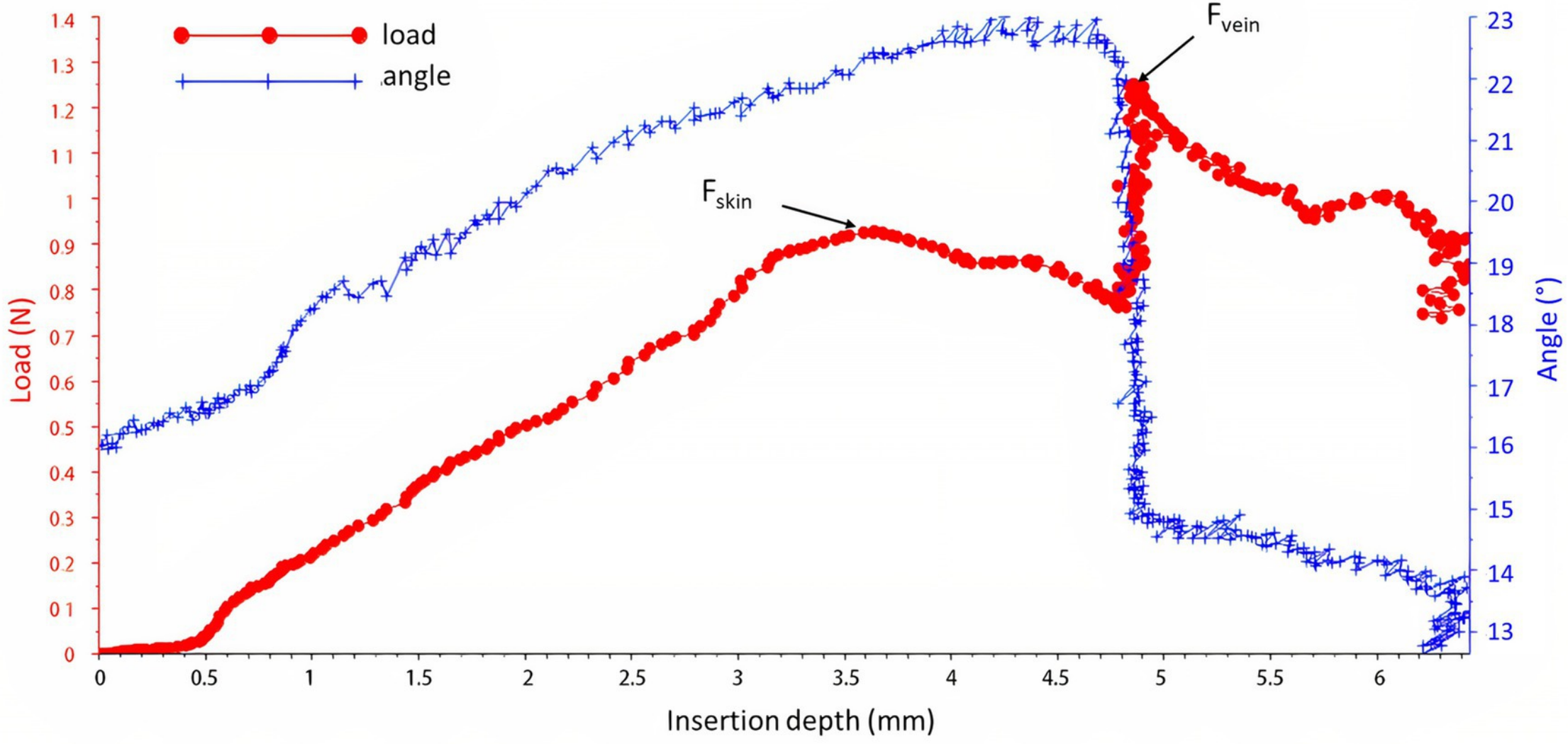
load
angle
F_{vein}
F_{skin}
Load (N)
Angle (°)
Insertion depth (mm)
0
0.1
0.2
0.3
0.4
0.5
0.6
0.7
0.8
0.9
1
1.1
1.2
1.3
1.4
13
14
15
16
17
18
19
20
21
22
23
0
0.5
1
1.5
2
2.5
3
3.5
4
4.5
5
5.5
6

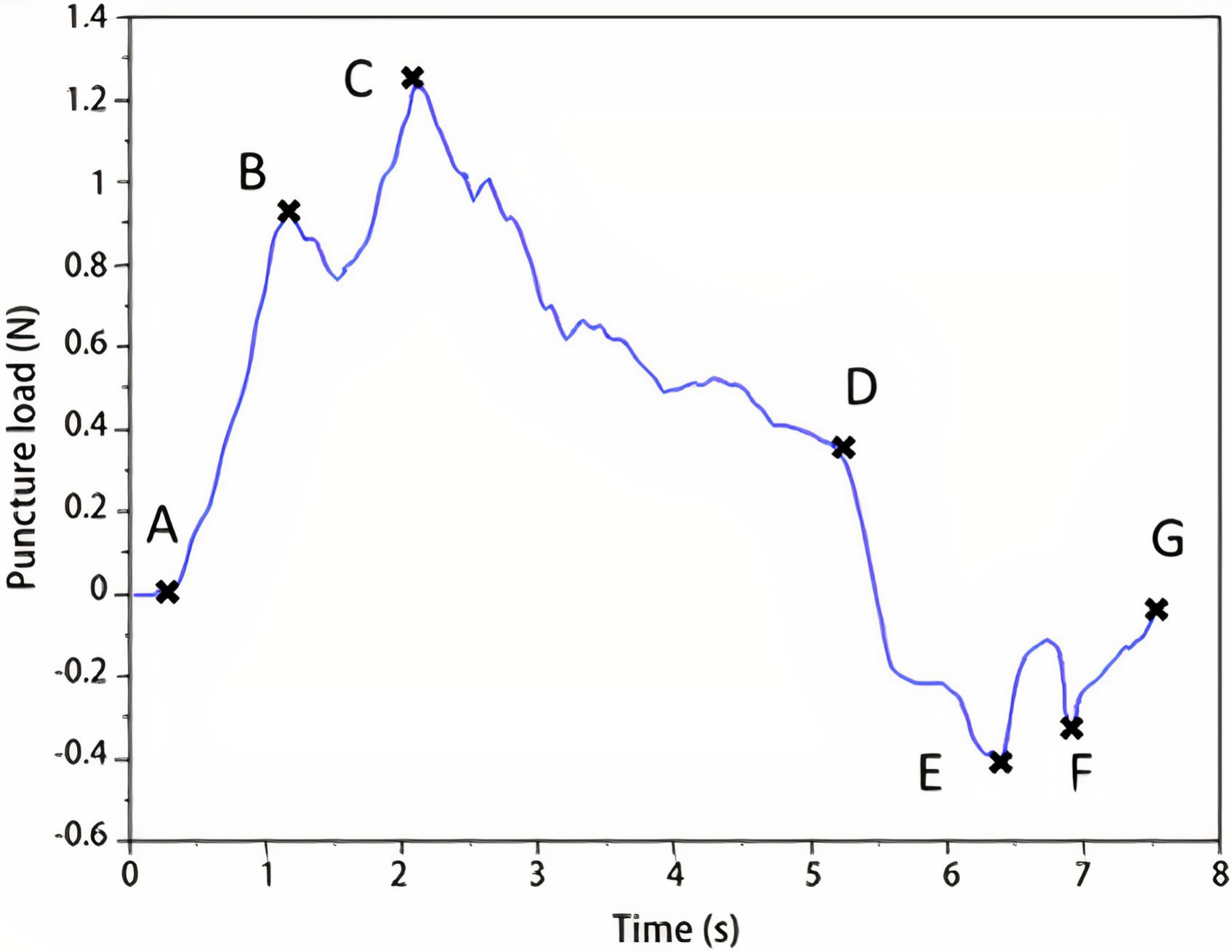
Puncture load (N)
1.4
1.2
1
0.8
0.6
0.4
0.2
0
-0.2
-0.4
-0.6
A
B
C
D
E
F
G
0
1
2
3
4
5
6
7
8
Time (s)

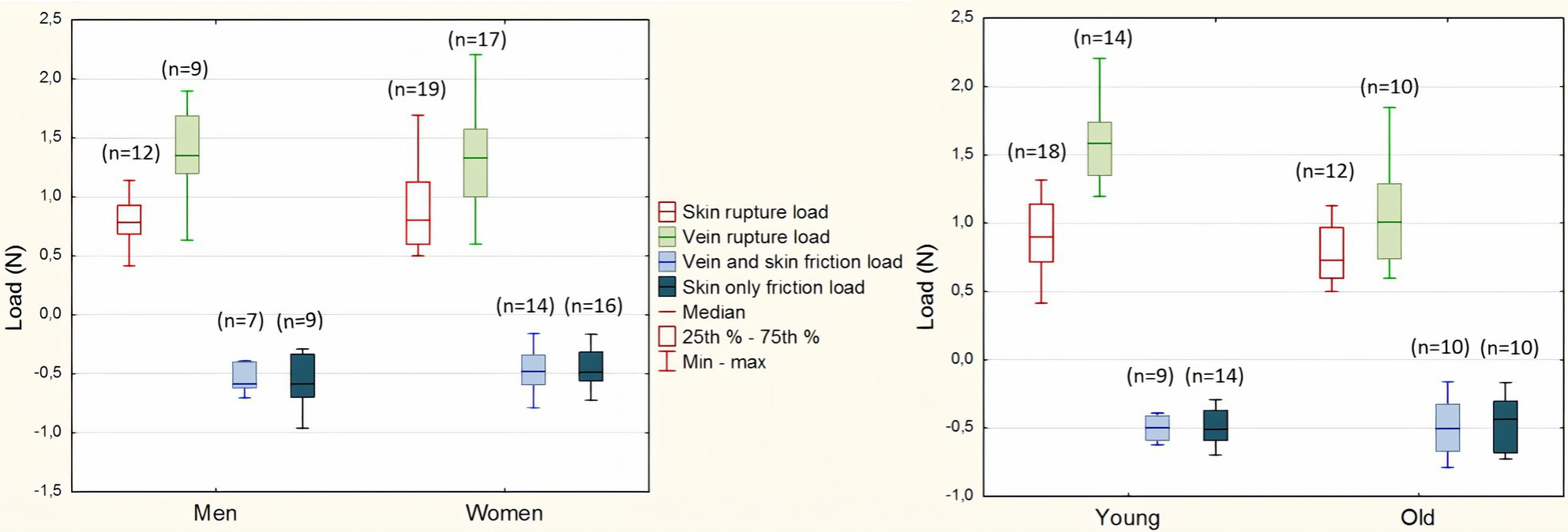
Load (N)
2,5
2,0
1,5
1,0
0,5
0,0
-0,5
-1,0
-1,5
(n=12)
(n=9)
(n=7)
(n=9)
(n=19)
(n=17)
(n=14)
(n=16)
Men
Women
Skin rupture load
Vein rupture load
Vein and skin friction load
Skin only friction load
Median
25th % - 75th %
Min - max
Load (N)
2,5
2,0
1,5
1,0
0,5
0,0
-0,5
-1,0
(n=18)
(n=14)
(n=9)
(n=14)
(n=12)
(n=10)
(n=10)
(n=10)
Young
Old

a)

b)